Dynamic force microscopy of copper surfaces: Atomic resolution and distance dependence of tip-sample interaction and tunneling current

Ch. Loppacher,* M. Bammerlin, M. Guggisberg, S. Schär, R. Bennewitz, A. Baratoff, E. Meyer, and H.-J. Güntherodt
Institute of Physics, University of Basel, Klingelbergstrasse 82, CH-4056 Basel, Switzerland
(Received 15 February 2000; revised manuscript received 30 June 2000)

Atomic resolution images of Cu(111) and Cu(100) surfaces obtained in ultrahigh vacuum with a combined scanning tunneling (STM)/atomic force microscope (AFM) are presented. Scan lines recorded in the noncontact AFM mode and the constant current mode show enhanced corrugation similar to STM experiments. Frequency shift versus distance curves are analyzed to determine the forces between probing tip and sample using the force separation method. The short-range chemical forces are in good agreement with an exponential law. The decay lengths of these chemical forces are found to be twice as large as the decay length of the tunneling current, as predicted by a simple theoretical model. However, both lengths are significantly larger than expected for metallic adhesive interactions.

I. INTRODUCTION

Since the scanning tunneling microscopy (STM) measurements of Hallmark *et al.*[1] and of Wintterlin *et al.*[2] on close-packed (111) surfaces of Au and Al it became obvious that observed corrugation heights could not be explained without invoking special tip induced electronic effects.[3,4] Wintterlin *et al.* suggested that forces between probing tip and sample may play an essential role in the image formation, in particular that the frontmost end of the tip is elastically deformed by adhesive forces. Improved resolution was observed after elongations of the probing tip caused by applied voltage pulses. This was interpreted in terms of a transfer of sample material to the tip, corresponding to the formation of a nanometer-sized metallic cluster on the tip. Dürig *et al.*[5] measured a metallic adhesion force gradient during tunneling operation between an Ir tip and an Ir surface and found an exponential decay of the interaction force in agreement with theoretical models. The measured decay length of $\lambda_T = 0.05$ nm for the tunneling current is in good agreement with the work function of 4–5 eV and results by Berndt *et al.*[6] on Cu(111) and Rose *et al.*[7] For the experiments of Dürig *et al.* with small oscillation amplitudes a decay length for the force $\lambda_F \simeq \lambda_T$ was found. Later, Dürig *et al.* studied the decay length of chemical forces above Au and Al and found larger values than expected.[8] This was explained by the authors by assuming a sample atom at the probing Ir tip. Recently Clarke *et al.*[9] compared corrugation heights from STM measurements on Cu(100) as a function of distance. The comparison of their data for the sharpest tips with molecular dynamics calculations describing sample and tip deformations confirmed the suggestion of Wintterlin *et al.* that forces play an important role in the image formation, and yielded useful estimates of involved forces.

Since the invention of the atomic force microscope (AFM) by Binnig *et al.*,[10] it was evident that AFM should in principle be the ideal tool to investigate short-range forces on the atomic scale. However, the lateral resolution in contact mode was found to be limited to some nanometers. After the noncontact AFM measurements by Giessibl[11] on Si(111)7 $\times$7 true atomic resolution has been achieved by AFM under ultrahigh vacuum on surfaces of different materials. Bammerlin *et al.*[12] demonstrated true atomic resolution on an insulator, NaCl(001), including the observation of point defects, whereas Loppacher *et al.*[13] and Orisaka *et al.*[14] presented true atomic resolution on a metal, Cu(111) and Ag(111), respectively, by noncontact AFM.

In the present work, we report combined noncontact AFM and simultaneously recorded tunneling current measurements. Beyond the experiments summarized above, we could measure both atomic corrugation and distance dependence of interaction and tunneling current with the same technique. Atomic resolution images of Cu(111) and Cu(100), including point defects, are presented and compared with distance versus tunneling current and frequency shift curves to determine the interaction forces by the separation procedure presented by Guggisberg *et al.*[15] The results are discussed with respect to both earlier experiments and models for the relation between tunneling currents and forces.

II. EXPERIMENTS

The experiments were performed with an ultrahigh vacuum compatible STM/AFM system, which has been described elsewhere.[16] The silicon single crystals tips oriented along the [100] direction were microfabricated rectangular cantilevers.[17] The cantilever is oscillated with a constant amplitude at its resonance frequency, with typical values of $f_0 = 150-400$ kHz. All STM measurements were performed in the constant average current mode. Since the bandwidth of the tunneling current preamplifier is limited to 3 kHz, the observed current corresponds to the time average tunneling current $\overline{I_t}$. In the limit $A/\lambda_T \gg 1$, where λ_T is the decay length of the tunneling current and A is the amplitude of the tip oscillation, it can be shown using the perturbation approach first introduced by Giessibl[18] that the average current $\overline{I_t}$ is related to the current $I_t = I_0 \exp(-z/\lambda_T)$ at closest separation z by[19]

$$\overline{I_t} = I_0 \exp(-z/\lambda_T) \frac{1}{\sqrt{2\pi A/\lambda_T}}. \tag{2.1}$$

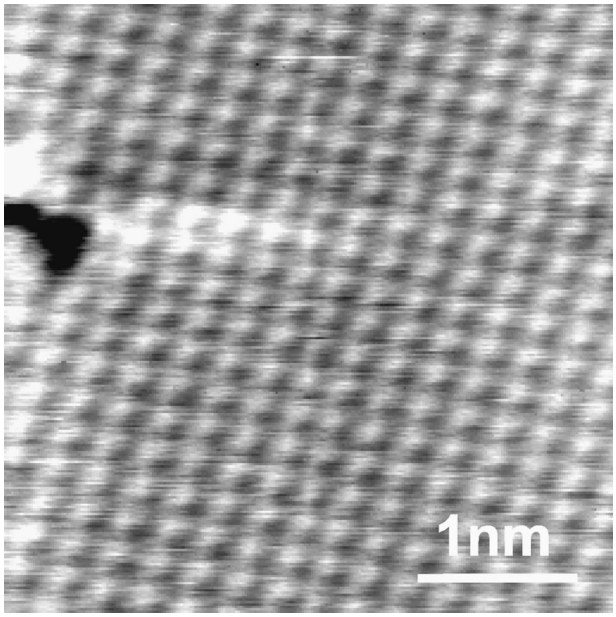

FIG. 1. Topographic image of Cu(100) at constant frequency shift $\Delta f = -47$ Hz, applied voltage $U_{sample} = 0.4$ V, resonance frequency $f_0 = 168$ kHz, oscillation amplitude $A = 1.5$ nm, corrugation height=13.5 pm.

Formula (2.1) is valid only for harmonic cantilever oscillations. Measurements of the frequency spectra at the closest point to the surface show that there is no significant distortion of the oscillation in the case of the large amplitudes used in our experiment. For a typical oscillation amplitude $A = 8$ nm and decay length $\lambda_T = 0.15$ nm, a tunneling current $I_t = 18 \times \overline{I_t}$ is found. In the noncontact AFM mode the frequency shift Δf of the cantilever that is induced by tip-sample interactions is measured with a digital phase-locked loop.[20] The topography-feedback regulates Δf to a constant preset value during scanning. A second feedback loop keeps the oscillation amplitude of the cantilever A constant by driving the cantilever support with a controlled amplitude A_{exc}.[21] The frequency shift can be related to the interaction force F by first-order perturbation theory:[18,22]

$$-\frac{\Delta f}{f_0} kA = \frac{1}{\pi}\int_0^{\pi} \cos(\varphi) F(z + A + A\cos(\varphi)) d\varphi, \quad (2.2)$$

where k is the spring constant of the cantilever ($k = 20-40$ N/m). The average force can be determined from experimental parameters as $\overline{F} = \Delta f k A / f_0$. The actual force at closest separation $F(z)$ can be calculated via Eq. (2.2) using explicit force versus distance laws. Alternatively, inversion formulas can be used as described by Dürig,[23] and by Hölscher *et al.*[24]

The Cu(100) and Cu(111) surfaces were prepared by repeated cycles of sputtering with 1 keV argon ions and of annealing to 850 K. The last annealing was restricted to 700K to reduce the sulfur concentration at the surface below the detection limit of our Auger spectrometer. A typical noncontact AFM image of Cu(100) is shown in Fig. 1. The measured lattice constant in the fast scan direction is 2.7 Å, close to the expected value of 2.55 Å. The frequency shift $\Delta f = -47$ Hz was kept constant, which corresponds to a constant average force of $\overline{F} = 13 \pm 2$ pN. The observed defect

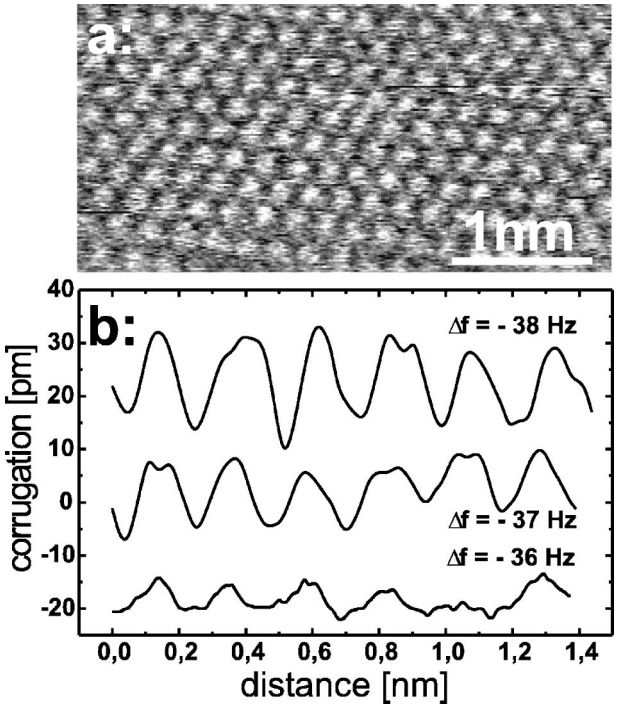

FIG. 2. Measurements at constant frequency shift on Cu(111). (a) topographic image at $\Delta f = -38$ Hz, $U_{sample} = 1.5$ V, $f_0 = 163$ kHz, $A = 25.5$ nm, corrugation height=17 pm; (b) line profiles through maxima showing the decreasing corrugation heights for less negative frequency shifts.

shows that the tip apex is as sharp as the best STM tips.[9] The corrugation height (peak to valley) is 13.5 pm. In order to measure a tunneling current, it was crucial to either sputter the tip or to run the instrument in contact mode for some minutes, which causes the decoration of the probing oxidized silicon tip by copper. The second procedure yielded copper terminated tips, as confirmed by frequency shift versus voltage curves (also called Kelvin force microscopy), where the minimum of the curve, corresponding to the contact potential difference between tip and surface, was found to be close to 0 V. Orisaka *et al.*[14] stated that it is crucial to compensate the contact potential between the tip and the surface to obtain atomic resolution. However, in our experiments we apply a voltage in order to measure tunneling current simultaneously. Furthermore, the additional attractive electrostatic forces shift the minimum of the frequency versus distance curve closer to the surface and, therefore, also the regime for stable feedback operation.[25] To further characterize the probing tip, I-V curves were performed, yielding a tunneling resistance of >10 GΩ and a nonlinear characteristic of the I-V curve in the regime where atomic corrugation is measured. The very high tunneling resistance indicates the existence of a second resistance in series to the tunneling gap. In our case the probing Si tip was probably covered by a thin oxide layer producing the additional resistance. Sputtered tips gave a significant contact potential difference, typically 1.0 V and lower tunneling resistances for the regime of atomic resolution. The copper terminated tip was used in a series of experiments where the corrugation height was measured as a function of frequency shift.

Figure 2(a) shows a representative topography image of the Cu(111) surface with an experimentally determined

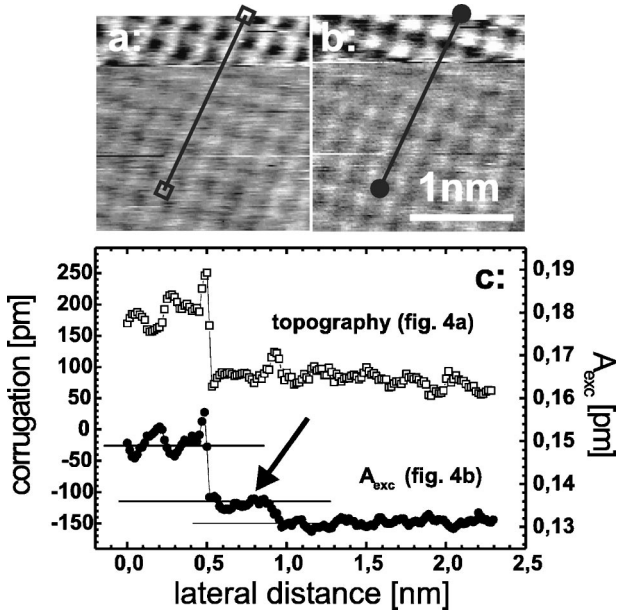

FIG. 3. Measurements at constant frequency shift $\Delta f = -73$ Hz on Cu(100), $U_{sample} = 0.4$ V, $f_0 = 168$ kHz, $A = 1.5$ nm. A tip change leads to an increased corrugation height from 16 pm to 39 pm in the upper part of the simultaneously recorded images; (a) topography and (b) excitation amplitude A_{exc} (line by line average). Line sections (raw data) along the line indicated in the images are shown in (c). The arrow shows a change in A_{exc} where the topography remains unchanged.

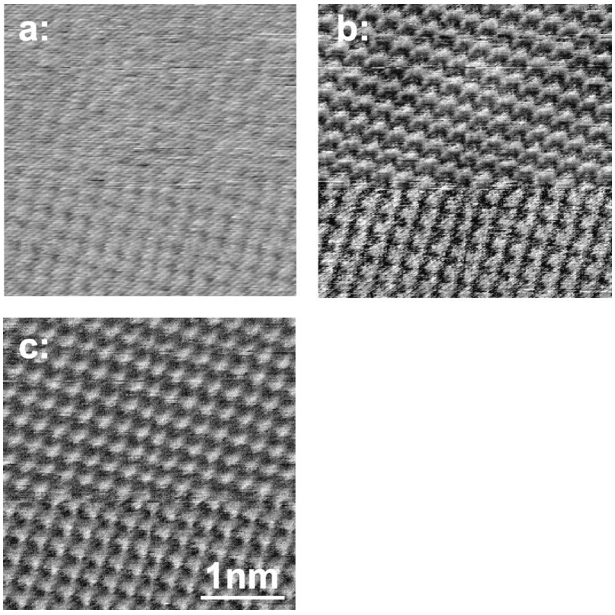

FIG. 4. Simultaneously recorded images at constant time-average current $\overline{I_t}$, $U_{sample} = 1.3$ V, $f_0 = 168$ kHz, $A = 6.5$ nm, $\overline{\Delta f} \simeq -70$ Hz. (a) topography, (b) frequency shift, (c) excitation amplitude A_{exc}. A tip change occurred about one-third of the way in the slow vertical scan direction.

atomic distance of 2.4 Å while the expected value for Cu(111) is 2.55 Å. Upon increasing the setpoint from $\Delta f = -36$ Hz to $\Delta f = -38$ Hz, corresponding to average forces $\overline{F}$ of 170 pN to 180 pN, the corrugation height in Fig. 2(b) is found to increase from 10 pm to 17 pm. The significant change of corrugation heights upon relatively small changes of the frequency shift can be explained by the contribution of the long-range forces to the frequency shift that are not directly involved in the formation of atomic contrast. As pointed out by Clarke *et al.*,[9] it is crucial that the tip itself does not change during such a set of experiments.

A comparison of these data with STM data of Clarke *et al.* on Cu(100), of Wintterlin *et al.* on Al(111), and of Berndt *et al.*[6] on the Cu(111) surface shows the same enhanced corrugation heights with similar distance dependence. Accidentally, it may happen that the tip suddenly changes as illustrated in the topography [Fig. 3(a)] and the A_{exc} [Fig. 3(b)] images of Cu(100). In this case, an increase of the corrugation from 16 pm to 39 pm is observed. Similar changes in corrugation height were attributed by Clarke *et al.*[9] to two distinct types of tips. The authors suggested that the tip yielding the smaller corrugation may have a metallic apex atom, whereas the other tip yielding the larger corrugation may be terminated by a nonmetal tip, e.g., a sulfur impurity atom picked up from the copper surface. Alternatively, Clarke *et al.* suggested that changes of corrugation are not related to changes of the apex species, but rather to differences of the tip apex geometry. The atomistic character of the tip changes in Fig. 3 is confirmed by a section through the topography plotted in Fig. 3(c). After the change, the topography baseline changes by only 0.11 nm. Surprisingly, the A_{exc} signal is even more sensitive to small tip changes that do not affect the corrugation height. Note further that A_{exc} is maximum at the minima of the topography as observed on NaCl(001).[12] However, increased forces are not necessarily in registry with the positions of the atoms as pointed out by Ciraci *et al.*[26] This inverted contrast and the short-range character of the A_{exc} signal are the subject of ongoing work and will be discussed elsewhere.

Besides the frequency shift feedback the Cu(100) surface was also atomically resolved using tunneling current feedback. Figure 4 shows simultaneously recorded topography, frequency shift Δf, and A_{exc} images of the Cu(100) surface. The corrugation in topography is 25 pm and shows a decreased resolution after a tip change in the lower part. Both the frequency shift and the A_{exc} signal show a clear contrast. Note that the contrast in Δf visualizes different distance dependencies of tunneling current and force, which will be analyzed below. After the tip change, atoms appear elongated with a ''peanutlike'' structure. This effect is quite typical for tip artifacts in STM or noncontact AFM on the atomic scale. Remarkably, the change of the shape of the atoms observed by the simultaneously acquired tunneling current is different. Due to these tip-related changes of the atomic contrast it is difficult to determine a phase relation between maxima and minima of tunneling current, force, and A_{exc}, respectively.

Having established true atomic resolution in both noncontact AFM and STM modes, we recorded frequency and average tunneling current versus distance curves. As shown in Fig. 5, an exponential variation of the average tunneling current is found with decay length of $\lambda_T = 0.15$ nm. The analysis of the frequency shift versus distance curves is more complicated, because of unavoidable long-range forces. Electrostatic forces can be minimized by compensating the contact potential difference with the applied sample bias voltage. As described by Guggisberg *et al.*,[15] short-range chemical forces can be separated by subtracting the long-range van der

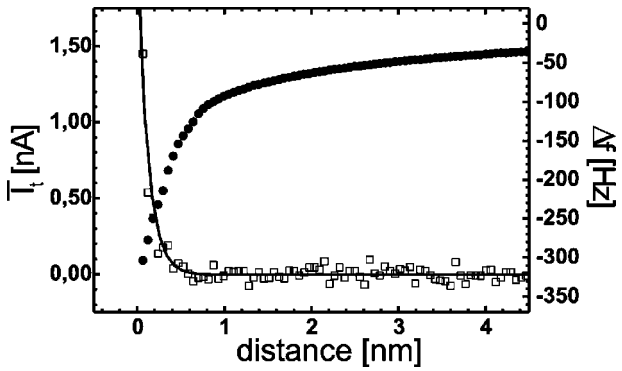

FIG. 5. Frequency shift Δf (dots) and time-average current $\overline{I_t}$ (squares) versus distance simultaneously recorded on Cu(100) for $U_{sample}=0.9$ V, $f_0=147$ kHz, $A=4.4$ nm. The solid curve shows an exponential fit with a decay length of $\lambda_T=0.15$ nm.

Waals contribution, which is done by fitting $\log \Delta f$ versus $\log z$ curves. A slope of -1.5 is found, which validates the model of a spherical mesoscopic tip end for the long-range van der Waals forces over distances smaller than its radius. Using a Hamaker constant of $A_H=4\times10^{-19}$ J, a tip radius of 10 nm is determined from the fit of the long-range part of the data ($z>2$ nm) (cf. Fig. 6). Upon subtraction the contribution of the short-range chemical force to Δf is revealed, as shown in Fig. 7. The absolute distances are calculated from the steep onset of the short-range A_{exc} signal, which is a clear indication of imminent contact.[27] The curve extends into the negative gradient regime, which is usually avoided to prevent tip changes. In the positive gradient range the short-range force varies exponentially with a decay length of $\lambda_F=0.31$ nm, which is a factor of 2 larger than the decay length of the tunneling current. An absolute determination of the short-range force done with Eq. (2.2) assuming a Morse potential is shown in the inset of Fig. 7. From the operation parameters, which ensure true atomic resolution and the fits shown in Fig. 7, we conclude that the optimum conditions are for frequency shift setpoints close to the minimum of the frequency shift versus distance curve, which corresponds to an attractive short-range force in the order of 0.5 nN as can be seen from the inset in Fig. 7. Similar values were previously predicted for atomically sharp tips by the combined

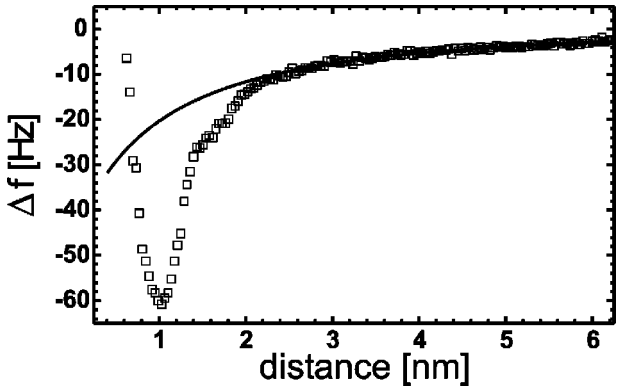

FIG. 6. Frequency shift Δf versus distance (squares) recorded upon approach to Cu(100) together with a van der Waals fit to the long-range part (solid curve); $U_{sample}=0.0$ V, $f_0=168$ kHz, $A=6.5$ nm.

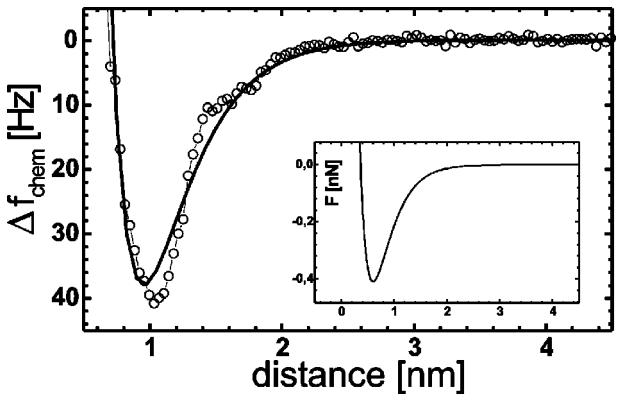

FIG. 7. Short-range contribution to the frequency shift Δf_{chem} (circles) determined upon subtraction of van der Waals contribution (Fig. 6). The inset shows the corresponding short-range force $F=2U_0/\lambda_F\{\exp[-2(z-z_0)/\lambda_F]-\exp[-(z-z_0)/\lambda_F]\}$, whereas the solid line shows Δf_{chem} computed for a Morse interaction potential with the fitted parameters $U_0=0.5$ eV and $\lambda_F=0.3$ nm.

STM measurements and molecular dynamics calculations of Clarke *et al.* for Cu(100) and the first-principles calculations of Ciraci *et al.* for Al(111).[26]

III. DISCUSSION

The most striking observations of our study are as follows:

(i) The achievement of true atomic resolution on the two most close-packed surfaces of a fcc metal in two dynamic modes possible with a combined AFM/STM,

(ii) The exponential decay of the short-range attractive tip-sample interaction and of the time-averaged tunneling current with respective decay lengths satisfying $\lambda_F=2\lambda_T$ down to distances where atomic resolution is possible,

(iii) The surprisingly large values of λ_T and λ_F, compared to values in the range 0.04 to 0.07 nm previously obtained in STM measurements with metallic tips[1,2,6,9] and in the approximate embedded-atom theory of bonding between metals invoked to explain deviations induced by tip-sample forces.[9,28] Similar values were obtained and a similar theory was used to interpret the first simultaneous measurements of tunneling current and force gradient on a metal.[5]

Regarding point (i), the observed corrugation heights, comparable to those obtained in the above-mentioned STM measurements, suggest that our measurements at constant $\overline{I_t}$ are performed at similar minimum tip-sample separations d. On the other hand, the corrugations of the electron density predicted in the relevant distance range above close-packed metal surfaces by the theories mentioned under point (iii), as well as by more accurate self-consistent calculations on which they are based, are one to two orders of magnitude smaller. Therefore our observations of much larger corrugations at constant frequency shift, i.e., approximately at constant force for oscillation amplitudes A much larger than d,[18] are incompatible with theories attempting to relate metallic adhesion forces to the electron density in the absence of the tip. Either such theories are inadequate for our purposes, or the tip induces site-dependent modifications of electronic structure, which in turn result in enhanced lateral variations of electronic overlap and of interaction forces between the

nominally flat sample and the tip.[3]

The relation mentioned under item (ii) has been proposed by Chen[29] by analogy with the molecular orbital picture of molecular bonding. For a tip-sample system in close proximity, the gain in binding energy ΔE due to weak overlap between electronic states of each subsystem is proportional to an average transition matrix element M. This quantity has an exponential dependence on the thickness s of the intervening potential barrier if s is larger than a few decay lengths, while s acquires a linear dependence on d, i.e., on the relative displacement of the sample. As a result, the force due to electronic overlap,

$$F = -\frac{\partial \Delta E}{\partial s} = \frac{\partial M}{\partial d} \tag{3.1}$$

is attractive and has an exponential dependence with the same decay length λ_F. On the other hand, in the same range, the tunneling current I_t is proportional to a weighted average of $|M|^2$ over the energy window defined by the voltage drop across the barrier.[30,4] Thus one expects $\lambda_F = 2\lambda_T$. At smaller separations, the assumptions underlying this relation break down because the barrier collapses, the overlap becomes large, the conductance saturates, and the electronic attraction begins to be compensated by repulsion between atoms.[3] Olesen *et al.*[28] showed that an apparent exponential dependence of the tunneling current on tip or sample displacement, i.e., on d, can nevertheless persist up to contact, owing to a reduction of s by tensile deformations induced by the tip-sample attraction. This should result in a more rapid variation of the force versus d, resulting in an apparent $\lambda_F < 2\lambda_T$. In the same range Ciraci *et al.* approximately find $F \propto I_t$, i.e., $\lambda_F \approx \lambda_T$, neglecting deformations.[26] The uncertainty and the numerous factors affecting the absolute magnitude of the time-averaged tunneling current in our dynamic measurements with partially metal and/or oxide covered silicon tips prevent an accurate absolute determination of d. At present it is therefore difficult to judge whether the assumption of weak overlap leading to $\lambda_F \approx 2\lambda_T$ can be justified a priori in the distance range shown in Fig. 5, for instance.

Point (iii) raises a number of issues that merit further study. Whereas $\lambda_F = 0.3$ nm is surprisingly larger than the range of typical chemical interactions, $\lambda_T = 0.15$ nm implies an effective barrier height

$$\overline{\phi} = \hbar^2/(8m\lambda_T^2) = 0.42 \text{ eV}, \tag{3.2}$$

considerably lower than the average work function of copper surfaces and the barrier height inferred from quasistatic tunneling current versus distance measurements on Cu(111) (Ref. 6) and Cu(100) (Ref. 9). One common reason for considerably reduced barrier heights in such measurements is a repulsive contact with an area of the tip that contributes little to the tunneling current, e.g., with a relatively thicker oxide layer.[31] However, this should produce a positive contribution to the simultaneously recorded frequency shift with a d dependence uncorrelated with that of $\overline{I_t}$, for which there is no evidence in our measurements. Furthermore, the average barrier model[32] that adequately describes the I_t-U characteristics of metallic STM junctions at a fixed separation layer[33] implies a significant voltage dependence of the effective barrier height,

$$\overline{\phi} \approx \phi - e\frac{U - U_c}{2} \tag{3.3}$$

and hence of λ_T, for biases comparable to the barrier height ϕ at compensated contact potential. No appreciable voltage dependence of λ_T was, however, obtained by us for either polarity in the range $|U| < 0.8$ to 1.2 V in which we could observe a time-averaged $\overline{I_t}$ with an acceptable signal-to-noise ratio. Although the apparent lack of voltage dependence might be due to the limited useful range of U, the two preceding equations imply $\phi = 0.9$ eV for an applied bias voltage of 1 V, still a suspiciously low value. Together with Chens relation, these two equations furthermore imply that the short-range attractive force (not to be confused with the long-range electrostatic force) would also be voltage dependent. We therefore repeated the measurements shown in Fig. 7 in the range where Δf drops with decreasing d for applied biases between -1.2 and $+1.2$ V and applied the separation procedure mentioned in connection with Fig. 7. Contrary to expectations, the corresponding fits to the short-range attractive force showed only slight variations of λ_F between 0.38 and 0.29 nm. The above-mentioned contradictions suggest that some other effects, hitherto not considered, are at the origin of the unusually long decay lengths that can be inferred from combined dynamic STM/AFM measurements like ours.

IV. CONCLUSION

In summary, true atomic resolution in two dynamic modes has been demonstrated on Cu(111) and Cu(100) surfaces with a combined STM/AFM in UHV. Contrary to expectations based on the behavior of the total electron density above the free surfaces, the corrugation heights and their distance dependence are comparable to previous STM measurements. Correlated contrast has been detected in simultaneously recorded images of the excitation amplitude that maintains a constant tip oscillation, in particular. Metallic adhesion forces with the presumably Cu-coated tip apex were determined quantitatively by a systematic procedure, in which electrostatic and van der Waals contributions were first subtracted.[15] In accordance with previous theoretical calculations for atomically sharp model tips, metallic adhesion forces of the order of 1 nN are inferred in the distance range where atomic resolution is obtained. In agreement with previous independent measurements, the short-range metallic forces decay exponentially with a decay length $\lambda_F = 0.31$ nm. The simultaneously recorded tunneling current also decays exponentially with a length of $\lambda_T = 0.15$ nm, in agreement with a simple theory by Chen. However, the underlying assumption of weak electronic overlap has been questioned in the range where attractive forces of the above-mentioned magnitude appear. Furthermore, compared to previous careful STM measurements with metallic tips on metal surfaces, the tunneling barrier height inferred from the decay length λ_T is surprisingly low, viz., 0.4 vs 2 eV in the case of Cu(100). Such a low barrier height is expected to be effectively decreased by the applied voltage; no significant depen-

dency of either λ_F or λ_T could be established, however. In conclusion, a close relationship between metallic adhesion and tunneling could be established down to distances where true atomic resolution is achieved, but the origin of the long decay lengths remains an issue that merits further studies.

ACKNOWLEDGMENT

This work was supported by the Swiss Priority Program MINAST, Kommission für Technologie und Innovation, and the Swiss National Science Foundation.

*Email address: Loppacher@iapp.de

[1] V.M. Hallmark, S. Chian, J.F. Rabolt, J.D. Swalen, and R.J. Wilson, Phys. Rev. Lett. **59**, 2879 (1987).
[2] J. Wintterlin, J. Wiechers, H. Brune, T. Gritsch, H. Höfer, and R.J. Behm, Phys. Rev. Lett. **62**, 59 (1989).
[3] S. Ciraci, E. Tekman, A. Baratoff, and I.P. Batra, Phys. Rev. B **46**, 10 411 (1992).
[4] C.J. Chen, *Introduction to Scanning Tunneling Microscopy* (Oxford University Press, New York, Oxford, 1992), Chap. 2.
[5] U. Dürig, O. Züger, and D.W. Pohl, Phys. Rev. Lett. **65**, 349 (1990).
[6] R. Berndt, J.K. Gimzewski, and R. Schlittler, Ultramicroscopy **42-44**, 528 (1992).
[7] J.H. Rose, J.R. Smith, and J. Ferrante, Phys. Rev. B **28**, 1835 (1983).
[8] U. Dürig, O. Züger, L.C. Wang, and H.J. Kreuzer, Europhys. Lett. **23**, 147 (1993).
[9] A.R.H. Clarke, J.B. Pethica, J.A. Nieminen, F. Besenbacher, E. Laegsgaard, and I. Stensgaard, Phys. Rev. Lett. **76**, 1276 (1996).
[10] G. Binnig, C.F. Quate, and Ch. Gerber, Phys. Rev. Lett. **56**, 930 (1986).
[11] F.J. Giessibl, Science **267**, 68 (1995).
[12] M. Bammerlin, R. Lüthi, E. Meyer, A. Baratoff, J. Lü, M. Guggisberg, Ch. Gerber, L. Howald, and H.-J. Güntherodt, Probe Microscopy **1**, 3 (1997).
[13] Ch. Loppacher, M. Bammerlin, M. Guggisberg, F. Battiston, R. Bennewitz, S. Rast, A. Baratoff, E. Meyer, and H.-J. Güntherodt, Appl. Surf. Sci. **140**, 287 (1999).
[14] S. Orisaka, T. Minobe, T. Uchihashi, Y. Sugawara, and S. Morita, Appl. Surf. Sci. **140**, 243 (1999).
[15] M. Guggisberg, M. Bammerlin, Ch. Loppacher, O. Pfeiffer, A. Abdurixit, V. Barwich, R. Bennewitz, A. Baratoff, E. Meyer, and H.-J. Güntherodt, Phys. Rev. B **61**, 11 151 (2000).
[16] L. Howald, E. Meyer, R. Lüthi, H. Haefke, R. Overney, H. Rudin, and H.-J. Güntherodt, Appl. Phys. Lett. **63**, 117 (1993).
[17] Nanosensors GmbH, Wetzlar, Germany; $0.01-0.02\ \Omega$ m *n*-doped silicon cantilever.
[18] F.J. Giessibl, Phys. Rev. B **56**, 16 010 (1997).
[19] F.J. Giessibl and H. Bielefeldt, Phys. Rev. B **61**, 9968 (2000).
[20] Ch. Loppacher, M. Bammerlin, F.M. Battiston, M. Guggisberg, D. Müller, H.R. Hidber, R. Lüthi, E. Meyer, and H.-J. Güntherodt, Appl. Phys. A: Mater. Sci. Process. **66**, S215 (1998).
[21] Excitation amplitude A_{exc}: output of the second feedback that keeps the amplitude constant. This signal is often referred to as the damping signal since any energy dissipation in the tip-sample interaction has to be compensated by an increase of A_{exc}.
[22] This relation, valid if $\Delta f/f_0$ is small, is most easily derived taking the first Fourier component of the tip treated as a harmonic oscillator subject to the force $F(z(t))$, where $z(t) \simeq z + A(1 + \cos 2\pi f_0 t)$.
[23] U. Dürig, Appl. Phys. Lett. **75**, 433 (1999).
[24] H. Hölscher, W. Allers, U.D. Schwarz, A. Schwarz, and R. Wiesendanger, Phys. Rev. Lett. **83**, 4780 (1999).
[25] M. Bammerlin, R. Lüthi, E. Meyer, A. Baratoff, J. Lü, M. Guggisberg, Ch. Loppacher, Ch. Gerber, and H.-J. Güntherodt, Appl. Phys. A: Mater. Sci. Process. **66**, S293 (1998).
[26] S. Ciraci, A. Baratoff, and I.P. Batra, Phys. Rev. B **42**, 7618 (1992).
[27] Our experiments show a steep onset of the A_{exc} signal similar to that of the tunneling current $\overline{I_t}$. For experiments without measured $\overline{I_t}$ we use the A_{exc} signal onset to additional 20% to define the separation between the closest point of the oscillation cycle and the sample to 4 Å.
[28] L. Olesen, M. Brandbyge, M.R. Sørensen, K.W. Jacobsen, E. Laensgaard, I. Stensgaard, and F. Besenbacher, Phys. Rev. Lett. **76**, 1485 (1996).
[29] C.J. Chen, *Introduction to Scanning Tunneling Microscopy* (Oxford University Press, New York, Oxford, 1992), Chap. 7.
[30] J. Bardeen, Phys. Rev. Lett. **6**, 57 (1960).
[31] J.M. Coombs and J.B. Pethica, IBM J. Res. Dev. **30**, 455 (1986).
[32] J.G. Simmons, J. Appl. Phys. **34**, 1793,2581 (1963).
[33] J.M. Coombs, M.E. Welland, and J.B. Pethica, Surf. Sci. **198**, L353 (1988).